Non-volatile ionic modification of the Dzyaloshinskii Moriya Interaction

L. Herrera Diez, Y Liu, D. Gilbert, M. Belmeguenai, Jan Vogel, S. Pizzini, E. Martinez, A. Lamperti, J B Mohammedi, A Laborieux, et al.

Non-volatile ionic modification of the Dzyaloshinskii Moriya Interaction

L. Herrera Diez,[1,*] Y.T. Liu,[1] D. A. Gilbert,[2,3] M. Belmeguenai,[4] J. Vogel,[5] S. Pizzini,[5] E. Martinez,[6] A. Lamperti,[7] J. B. Mohammedi,[8] A. Laborieux,[1] Y. Roussigné,[4] A. J. Grutter,[2] E. Arenholtz,[9] P. Quarterman,[2] B. Maranville,[2] S. Ono,[10] M. Salah El Hadri,[11] R. Tolley,[11] E. Fullerton,[11] L. Sanchez-Tejerina,[12] A. Stashkevich,[4] S. M. Chérif,[4] A. D. Kent,[8] D. Querlioz,[1] J. Langer,[13] B. Ocker,[13] and D. Ravelosona[1]

[1]*Centre de Nanosciences et de Nanotechnologies, CNRS, Univ. Paris-Sud, Université Paris-Saclay, C2N Palaiseau, 91120 Orsay cedex, France*
[2]*NIST Center for Neutron Research, National Institute of Standards and Technology, Gaithersburg, Maryland 20899, USA.*
[3]*Department of Materials Science and Engineering, University of Tennessee, Knoxville, Tennessee 37919, USA.*
[4]*Laboratoire des Sciences des Procédés et des Matériaux, CNRS-UPR 3407, Université Paris 13, Sorbonne Paris Cité, 93430 Villetaneuse, France.*
[5]*Univ. Grenoble Alpes, CNRS, Institut Néel, 38000 Grenoble, France.*
[6]*Departamento de Física Aplicada, Universidad de Salamanca, Plaza de la Merced s/n. 37008 Salamanca, Spain*
[7]*IMM-CNR, Unit of Agrate Brianza,, Via C. Olivetti 2, 20864 Agrate Brianza (MB), Italy.*
[8]*Department of Physics, New York University, New York, New York 10003, USA.*
[9]*Advanced Light Source, Lawrence Berkeley National Laboratory, Berkeley, California 94720, USA.*
[10]*Central Research Institute of Electric Power Industry, Yokosuka,Kanagawa 240-0196, Japan.*
[11]*Center for Memory and Recording Research, University of California, San Diego, La Jolla, California 92093-0401, USA*
[12]*Dpto. Electricidad y Electronica, University of Valladolid, 47011 Valladolid, Spain*
[13]*Singulus Technology AG, Hanauer Landstrasse 103, 63796 Kahl am Main, Germany.*

The possibility to tune the Dzyaloshinskii Moriya interaction (DMI) by electric (E) field gating in ultra-thin magnetic materials has opened new perspectives in terms of controlling the stabilization of chiral spin structures. Most recent efforts have used voltage-induced charge redistribution at the interface between a metal and an oxide to modulate DMI. This approach is attractive for active devices but it tends to be volatile, making it energy demanding, and it is limited by Coulomb screening in the metal. Here we have demonstrated the non-volatile E-field manipulation of DMI by ionic liquid gating of Pt/Co/HfO_2 ultra-thin films. The E-field effect on DMI scales with the E-field exposure time and is proposed to be linked to the migration and subsequent anchoring of oxygen species from the HfO_2 layer into the Co and Pt layers. This effect permanently changes the properties of the material showing that E-fields can not only be used for local gating in devices but also as a highly scalable materials design tool for post-growth tuning of DMI.

I. INTRODUCTION

Controlling magnetic states in ferromagnetic metals by electric (E) fields [1] is a promising route for lowering power consumption in spintronics devices. Lowering critical switching currents in magnetic tunnel junctions [2] and improving domain wall motion in race-track devices [3] by inducing E-field anisotropy modulations are among the most exciting perspectives. The Dzyaloshinskii Moriya interaction (DMI) has also revealed itself as a key element in the design of novel spintronics devices since it can induce the formation of chiral magnetic structures like skyrmions and Néel like domain walls [4]. Controlling DMI by E-fields is therefore of outstanding practical interest since it could allow for the dynamic and local tuning of chiral spin structures.

E-field control of magnetic anisotropy and domain wall (DW) dynamics through a pure charge accumulation [5–9] or an ionic motion mechanism [6, 9–13] have been demonstrated, the non-volatility of ionic effects making them particularly interesting for applications. E-field control of DMI has been recently observed through volatile charge accumulation in CoFeB/TaO_x [14] and Pt/Co/Pd [15] systems. In addition, a reported E-field induced modulation of skyrmion bubble nucleation in Pt/Co/Al_2O_3 [16] indicates also a potential E-field effect on DMI. In terms of ionic effects on DMI, evidence has been shown indirectly as the ionic control of the spin Hall angle [17] in Pt/Co/GdO_x systems. However, a detailed characterisation of the effects of E-field induced ionics on DMI and an assessment of the full potential of ionics in defining the magnitude of DMI in a non-volatile fashion is still lacking.

In this study we present a non volatile and cumulative E-field induced reduction of DMI in Pt/Co (0.6 nm)/HfO_2/ionic liquid (IL) gate devices which is accompanied by a spin reorientation transition (SRT) from in-plane to perpendicular magnetic anisotropy (PMA). These E-field induced changes have been related to the migration of oxygen species from HfO_2 into the Co and Pt layers producing a gentle oxidation of the

*Electronic address: liza.herrera-diez@c2n.upsaclay.fr

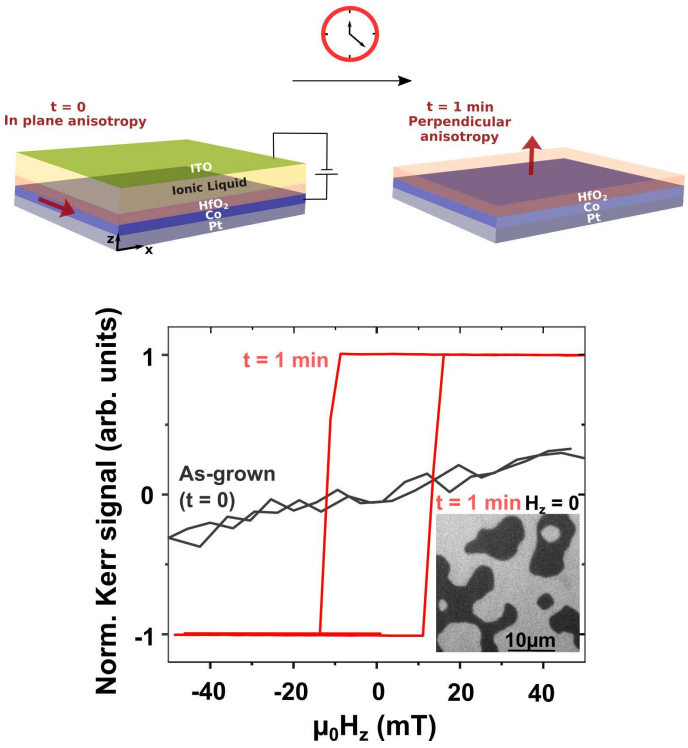

FIG. 1: Schematic of the Pt/Co/HfO_2 liquid gate device together with hysteresis loops measured under a perpendicular magnetic field before (black) and after (red) applying a gate voltage of -3V for 1 minute. The Kerr microscopy image (inset) shows the domain pattern in the demagnetised state after the gate voltage application.

Co and important structural changes at the interfaces. Oxidation at the Co/HfO_2 interface is thought to be responsible for the increase (and subsequent decrease at long biasing times) in PMA while Co oxidation and ion recombination at the Pt/Co interface is thought to lead to a decoupling between the Pt and Co layers and in turn, a weakening of the DMI.
It is worth noting that the liquid gate [18] can be removed after these non-volatile effects have been induced, opening the possibility of using E-fields as a low-cost and simple tool for materials design.

II. MAGNETISATION, PERPENDICULAR ANISOTROPY AND DMI

Figure 1 shows a schematic view of the device and the hysteresis loops measured under a perpendicular magnetic field corresponding to an as-grown film (black line) and a film exposed to a gate voltage of -3V (red line) for a duration of 1 minute. A full SRT into a perpendicular magnetic anisotropy state takes place and persists when the voltage and liquid gate are removed. All experiments have been conducted in ambient conditions and the bias voltage (-3V) was applied between the Pt layer and a top

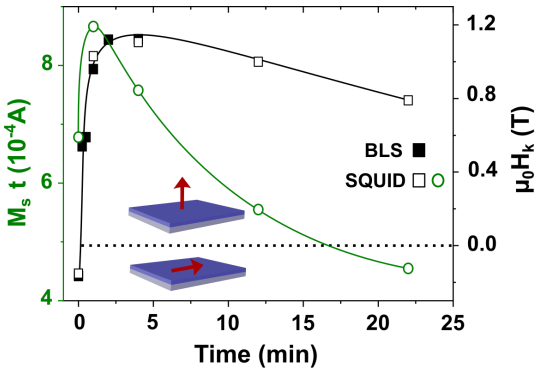

FIG. 2: (a) $M_s \times t$ (circles) and (b) $\mu_0 H_K$ (squares) as a function of the E-field biasing time. Lines are a guide to the eye.

counter electrode coated with transparent $InSnO_x$ (ITO) for 1 minute to 22 minutes. The resulting E-field at the surface of the film is approximately 0.6 GV/m (see supplementary information for more details [19]). Figure 2 shows the evolution of the measured product $M_s \times t$ (circles), where M_s and t are the saturation magnetisation and the film thickness, respectively. M_s was measured by superconducting quantum interference device (SQUID) magnetometry using out of plane magnetic field ramps going up to a saturation field of 600 mT and 120 mT for the as-grown and biased samples, respectively. Straight lines were subtracted from all loops to correct for the diamagnetic background. All of the film pieces were cleaved from the same wafer and have the same properties before E-field exposure. The anisotropy field $\mu_0 H_K$ measured by BLS (full squares) and SQUID (empty squares) as a function of the biasing time is also shown. $M_s \times t$ increases between 0 and 1 minutes followed by a monotonic decrease. The trend in $\mu_0 H_K$ suggests a weakening of the perpendicular magnetic anisotropy constant K_{eff} ($\mu_0 H_K = 2K_{\text{eff}}/M_s$, considering a constant $t = 0.6$ nm, see supplementary information [19]) beyond 4 minutes.
The values of the DMI constant strength D measured by BLS are shown in Fig. 3 (a) (full symbols). These values were obtained by analysing under a saturating in-plane magnetic field the frequency asymmetry (ΔF) of the BLS Stokes and anti-Stokes inelastic scattering peaks as a function of the wave vector k_{SW} [20] shown in Fig. 3 (b), a dependence ruled by the following expression:

$$\Delta F = \frac{2\gamma}{\pi M_s} D k_{SW}, \qquad (1)$$

where γ is the gyromagnetic ratio. Stokes and anti-Stokes peaks for an as-grown film and a film biased for 1 minute are shown in Fig. 3 (c) and (d), respectively (see supplementary information for the full dataset [19]). Solid lines correspond to a Lorenzian fitting of the peaks. The absolute DMI value presents a strong decrease between 0 and 1 minutes and tends to stabilise around D= -0.3 mJ/m^2 in the range between 2 minutes and 4 minutes. These values have been calculated using the measured

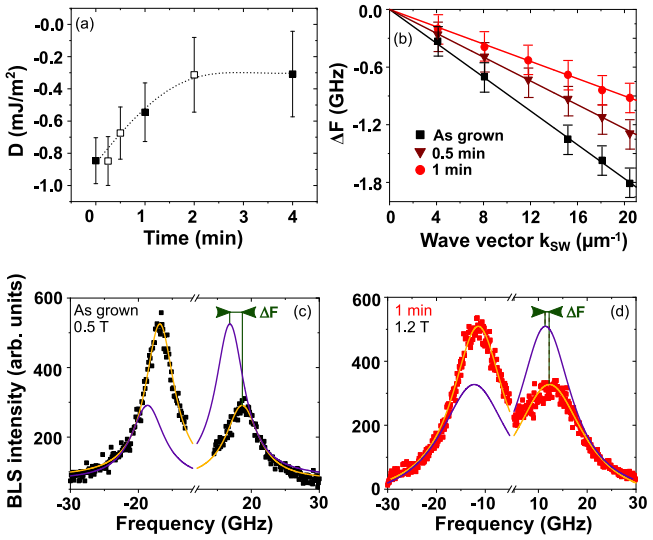

FIG. 3: (a) DMI constant D as a function of the biasing time, values calculated using estimated M_s values are shown as empty symbols. The dotted line is a guide to the eye. (b) Frequency asymmetry as a function of the wave vector and linear fitting lines. BLS spectra at $k_{SW} = 20\mu m^{-1}$ for the (c) as-grown and (d) 1 minute biased films. The solid lines correspond to the Lorenzian fitting.

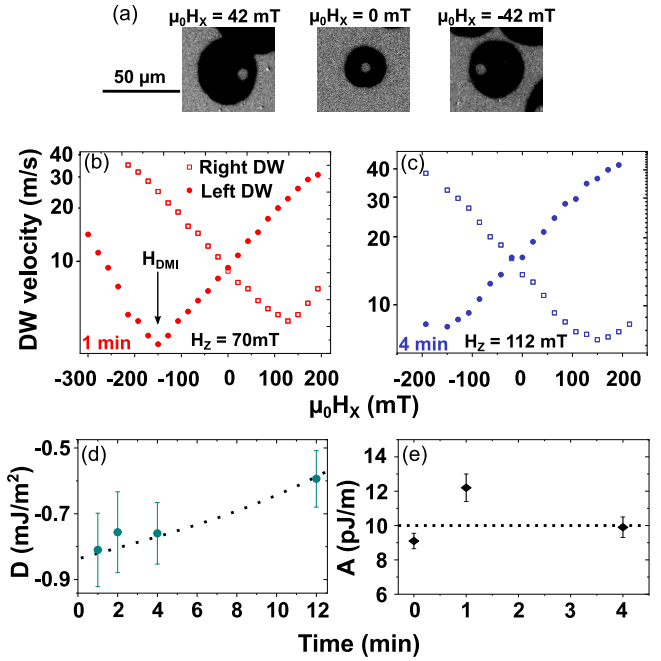

FIG. 4: (a) Kerr microscopy images of the domain expansion in the sample biased for 1 minute under in-plane fields ($\mu_0 H_X$). Velocity curves as a function of $\mu_0 H_X$ from films biased for 1 (b) and 4 (c) minutes, respectively. (d) DMI parameter D extracted using the experimentally obtained values of A shown in (e). Lines are a guide to the eye.

$M_s \times t$ values presented in Fig. 2 (full symbols) or an estimation based on the same data set (empty symbols) and considering the nominal Co layer thickness of 0.6 nm. Potential E-field induced variations in t have been taken into account and do not modify significantly these results (see supplementary information [19]). Reversing the E-field polarity or removing the ionic liquid from the samples did not recover the values of DMI, M_s or $\mu_0 H_K$, indicating that the induced changes are permanent and irreversible (see supplementary information [19]). The total DMI variation presented here amounts to a factor of ≈ 2.9 with respect to the initial value which is significantly higher than the variations obtained by charge accumulation in both CoFeB/TaO$_o$ [14] and Pt/Co/Pd [15] systems, of nearly a factor of ≈ 2.2 and ≈ 1.1, respectively.

III. MAGNETIC DOMAIN WALL MOTION

The value of DMI can also be evaluated by measuring the asymmetry of magnetic DW motion under simultaneous in-plane and out of plane magnetic fields [21, 22] in the perpendicular anisotropy regime. Typical Kerr microscopy images of the magnetic domain asymmetric expansion under in-plane fields ($\mu_0 H_X$), a signature of the presence of DMI, in a film biased for 1 minute are presented in Fig. 4 (a). The velocity curves under $\mu_0 H_X$ for the films biased at 1 and 4 minutes (Fig. 4 (b) and (c), respectively) show minima at $\pm\mu_0 H_{DMI}$ that are correlated to the magnitude of the DMI parameter D:

$$\mu_0 H_{DMI} = \frac{D}{M_s \Delta}, \qquad (2)$$

where $\Delta = \sqrt{A/K_{\text{eff}}}$ is the domain wall width parameter and A the exchange stiffness constant [21] (see supplementary information for the full dataset [19]). D values have been calculated for biasing times of 1 minute, 2 minutes, 4 minutes and 12 minutes and are shown in Fig. 4 (d). The value of A used in these calculations was determined by measuring the temperature dependence of the magnetic moment for as-grown, 1 minute and 4 minute samples and evaluating the validity of the Bloch $T^{3/2}$ law [23, 24] (see supplementary information [19]). The values of A are shown in Fig. 4 (e), they vary between 9 pJ/m and 12 pJ/m which is below the typical value used for thin films (16 pJ/m [25, 26]). This difference can be attributed to the ultra-thin nature of the magnetic film [23] which could contribute to a more pronounced influence of alloying with Pt that has been shown to induce a decrease in A [26].

Although the D values measured by BLS and DW motion show a similar trend, the DW motion measurements give higher values and a weaker dependence on the E-field than those obtained by BLS. The origin of the discrepancies between these two sets of values remains an open question. Discrepancies between D values obtained by DW motion experiments under in-plane fields and BLS

have already been reported and attributed to the difference in length scales probed by each technique [21] or by the limitations of a simplified model in more complex scenarios [27]. In this context, an inhomogeneous D in the film could be responsible for the discrepancy. Since the mechanism for the modulation of D in this study is related to a modification of the material it can not be ruled out that the E-field effect has not only an impact on the average value of D but also on its distribution across the sample, for example through preferential ionic accumulation in the vicinity of a defect, which could increase a discrepancy between different measurement methods. Additionally, the calculation of the D values by DW motion measurements depends on the accuracy of the measured K_{eff} and A values, an uncertainty not present in the derivation of the D values by BLS and which could give rise to a discrepancy with the values obtained from DW motion.

Figure 5 (a) shows the DW velocity curves as a function of the perpendicular magnetic field strength obtained for biasing times of 1 minute, 2 minutes and 4 minutes (open symbols) indicating a strong reduction of the DW velocity consistent with the observed decrease in D. The curves do not present the typical dependence described by the one dimensional model of DW motion [28], namely a strong decrease of the speed after the Walker field, followed by a linear increase with low mobility, instead they show a saturation of the DW velocity a high magnetic fields. This feature, which has already been observed in a number of materials including Pt/Co [25, 29, 30], has been attributed to instabilities of the internal structure of the DW above the Walker field, where the annihilation of vertical Bloch lines allows maintaining high velocities after the Walker field [31].

Micromagnetic simulations conducted in order to better understand the mechanism behind the observed velocity reduction are also shown in Fig. 5 (a) (full symbols). The simulations were performed considering an area of 2μm $\times$ 2μm and a granular structure with a grain size of 20nm and a dispersion of K_{eff}, M_s and D in order to simulate disorder (see Fig. 5 (b) and supplementary information for more details [19]). The simulated disorder introduced here is based on the typical grain size values found in the literature for this type of material. The individual variation of the experimental parameters for each grain is introduced randomly in the 0-20% range which constitutes an average of 10%, also a typical value [27, 32]. The simulations presented in Fig. 5 (b) have been obtained with values of D of 1.3 mJ/m^2, 1.05 mJ/m^2 and 0.74 mJ/m^2 for the samples biased for 1 minute, 2 minutes and 4 minutes, respectively, which are significantly higher than the D values obtained by either BLS or DW motion. Other studies in the literature [30] have shown that intermixing and disorder at the ferromagnetic/heavy metal interface can not only lead to changes in D but can also have a large impact on the value of the DW velocity plateau. A careful analysis of the impact of E-field induced ionic motion on disorder is needed to complete the picture and better understand the discrepancies between the values of D obtained by different methods. Nevertheless, the decreasing trend of the DMI strength with respect to the exposure time is confirmed by all methods.

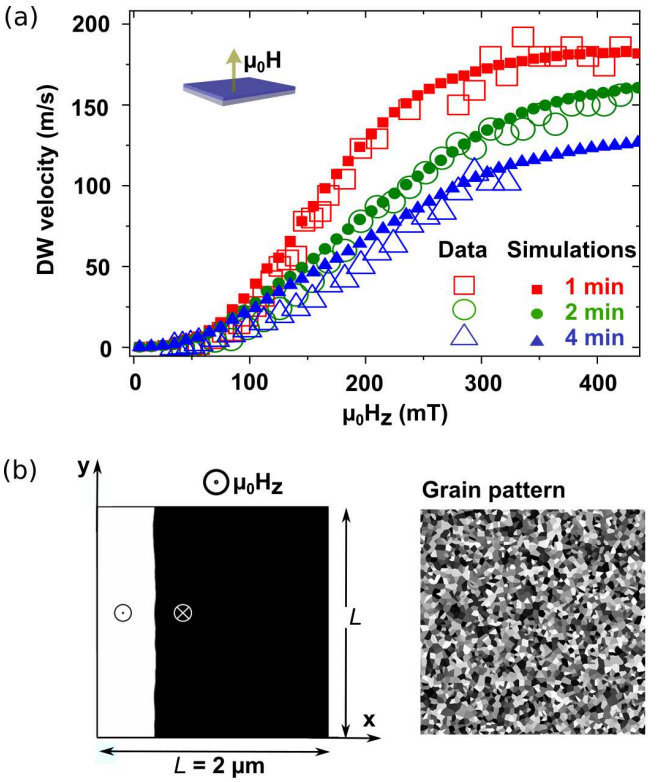

FIG. 5: (a) Experimental domain wall velocity as a function of a perpendicular magnetic field for films biased for 1 minute, 2 minutes and 4 minutes (empty symbols) and micromagnetic simulations (full symbols). (b) Granular structure used for the micromagnetic simulations.

IV. STRUCTURAL ANALYSIS

In order to elucidate the mechanism behind the E-field induced modification of the DMI strength we have conducted a thorough structural analysis to unveil the E-field effect on the structure of the interfaces and the oxidation state of Co. This has been done by conducting X-ray absorption spectroscopy (XAS), X-ray photoelectron spectroscopy (XPS) and polarised neutron reflectometry (PNR) experiments.

Figure 6 shows the XAS spectra in the energy range corresponding to the Co L_2 and L_3 edges of as-grown as well as samples biased for 1 minute, 2 minutes and 4 minutes. The known features corresponding to higher oxidation states in Co, namely satellite peaks at the L_3 edge that depend on the Co oxidation state [11, 33, 34], show as subtle variations in the symmetry of the main peak after biasing. However, the intensity of the L_3 peak increases significantly as a function of biasing time which

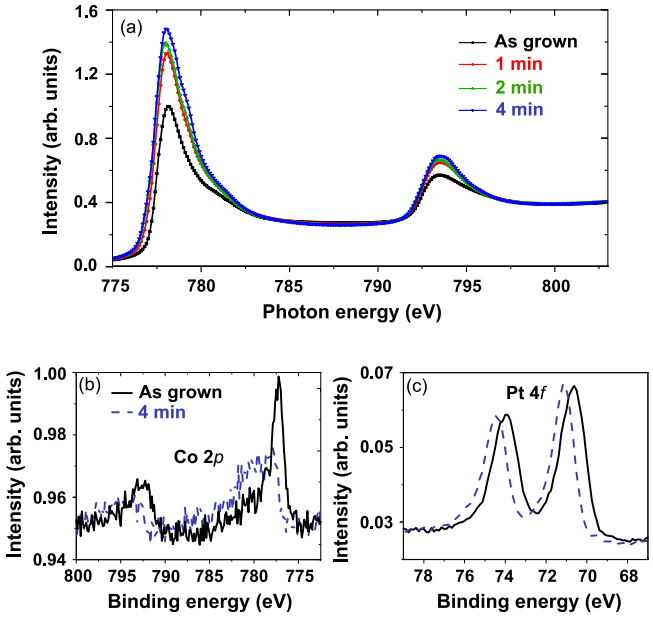

FIG. 6: (a) XAS spectra at the Co L_2 and L_3 edges as a function of the biasing time. XPS spectra at the (b) Co $2p_{3/2}$ and (c) Pt $4f$ regions for an as-grown sample (solid lines) and a sample biased for 4 minutes (dotted lines).

is an indication of an increase in unoccupied d levels [35] and could be correlated with a higher valence state in Co. The increase in the Co valence inferred by XAS is confirmed by the surface analysis provided by XPS and shown in Fig. 6 (b) and (c) for the as-grown sample (solid line) and a sample biased for 4 minutes (dotted line). A significant decrease in the intensity of the metallic Co $2p$ peaks and a shift towards higher binding energies confirm a change in the chemical environment in Co consistent with an increase in valence. A similar correspondence between the XAS and XPS profiles has been observed in the presence of mild oxidation in $Pt/Co/AlO_x$ layers [36].

Additionally, Fig. 6 (c) shows the intensity of the $4f$ peaks of Pt where also a clear shift to higher binding energies is observed. Studies in the literature have linked a similar increase in the binding energy to an interaction with oxygen species [37] which is in agreement with the oxidation signature in the Co spectrum. No significant changes in the Hf $4f$ and O $1s$ peaks have been observed (see supplementary information [19]).

Further insight into the E-field impact on interface structure is provided by PNR measurements. This technique allows for the construction of a depth profile of the magnetic and material characteristics of the system and provides a transverse characterisation of the interfaces [11, 12, 38, 39]. Figure 7 (a-c) shows a series of high-frequency Kiessig oscillations, with a second longer period structure, corresponding to the thick SiO_2 underlayer and thinner HfO_2, Pt and Co layers, respectively. The splitting between the spin-up and spin-down neutron channels (R^{++} and R^{--}, respectively) is qualitatively related to the in-plane projection of the magnetisation. The splitting is quantitatively presented in the spin asymmetry, defined as $SA \equiv (R^{++} - R^{--})/(R^{++} + R^{--})$, which is shown in Fig. 7 (d-f). A model incorporating the thickness, interface roughness, magnetic scattering length density (ρ_M, magnetic SLD) and nuclear SLD (ρ_N), of each of the layers is generated, then the reflectometry of the proposed structure is calculated and compared to the experimental data. Through an iterative feedback calculation a model is developed that accurately reproduces the experimental results. The models were fitted in parallel with coupled parameters, significantly improving the uniqueness of the converged fits.

The converged models presented in Fig. 7 (g-i) agree well with the expected profile, while the calculated scattering patterns, shown in solid lines for Fig. 7 (a-f), agree well with experimental measurements. Unexpectedly, the nuclear structure reveals a progressive broadening of the SiO_2/Pt interface, and an increase in the Pt thickness, but little change in the Pt SLD.

The ferromagnetic signature of Co obtained from PNR measurements gives further insight into the mechanics of the E-field indicating a marked surface oxidation of the Co. The magnetic profile was obtained measuring under an in-plane magnetic field (200mT) well below $\mu_0 H_k$ of the PMA phase. Under these conditions the as-grown sample is saturated in-plane and a proximity induced magnetisation in the Pt layer is observed. After the E-field treatment the magnetic signal in the plane of the sample is strongly reduced and it is concentrated at the Co/HfO_2 interface. This signal is the in-plane projection of the magnetisation and anisotropy effects can not be distinguished from changes in M_s. However, this reduction can be directly related to the spin reorientation transition evidenced by SQUID measurements where a large PMA is present in samples biased for 2 minutes and 4 minutes in contrast to the as-grown sample that is fully magnetised in-plane.

Considering the nuclear and magnetic profiles together, the initial magnetic SLD being lower than bulk and the nuclear SLD being larger suggests that the as-grown Co film may be partly oxidized. Assuming that the E-field simply induces the injection of OH^- or O^{-2} into the stack would decrease the magnetic SLD, but would raise the nuclear SLD, which is not observed. One possibility is that the E-field treatment might inject hydrogen ions in the form of OH^-. In this context, the Pt surface could act as a catalyst and promote the binding between oxygen ions and Co while inducing the irreversible anchoring of hydrogen ions to the Pt layer. This process could happen not only at the Pt/Co interface but also at the SiO_2/Pt interface which substantially broadens after the E-field treatment. At the Co/HfO_2 interface a stronger effect could be expected since it is in close vicinity of the OH^- source, the HfO_2 layer. Therefore, it is likely that the first atomic layer of Co is the one presenting the highest level of oxidation. This

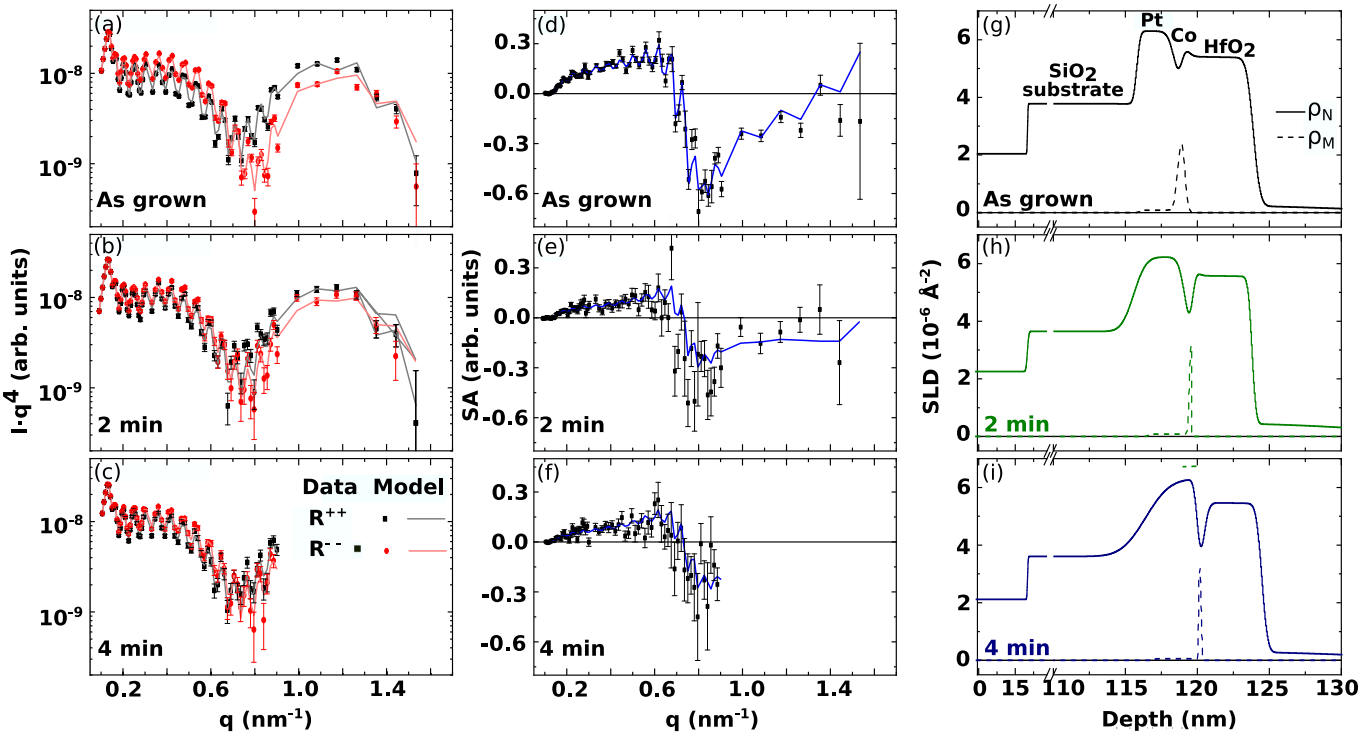

FIG. 7: (a-c) PNR signals R^{++} and R^{--} as a function of the wave vector and the corresponding fitting lines, the spin asymmetry is plotted in (d-f). The scattering length density (SLD),the model used to fit the experimental data, is presented in (g-i).

is supported by the SLD magnetic profile, showing a magnetisation in-plane component concentrated at this interface in PMA samples that could arise due to an over oxidation.

Ionic motion in HfO_2 and its interplay with ambient humidity provides a possible explanation for these findings. Studies in the literature have addressed the role of water incorporation into HfO_2 exposed to air and proposed that a dissociative adsorption of each water molecule at the HfO_2 surface can lead to the production of two OH^- ions [40, 41]. In addition, in samples where a subsequent selective removal of the HfO_2 layer is performed, a signature of labeled OH^- ions introduced through exposure to humidity is still present, and is linked to a migration and subsequent anchoring of OH^- to the SiO_2 substrate [40]. This scenario, where a preferential creation and migration of negatively charged species inside the HfO_2 layer can occur, has also a correspondence with the observed asymmetric response of the system to the E-field where no effects or reversibility are observed under positive gate voltages (see supplementary information [19]). In addition, the potential anchoring of these species at the SiO_2/Pt interface could account for the large increase in the interface width that is evidenced by PNR.

V. DISCUSSION

The results presented in the previous sections unveil a complex scenario where E-fields induce structural, chemical and magnetic changes across the whole SiO_2/Pt/Co/HfO_2 multilayer pointing at the role of ionic migration across multiple interfaces. Several studies in the literature relate E-field induced ionic effects at a Co/oxide interface to the migration of O^{-2} ions that can bind to the Co increasing its oxidation state [10, 11, 42]. Reports on Pt/NiCo/HfO_2/IL systems show reversible non-volatile voltage effects on the magnetic properties by long biasing times between 10 minutes and 60 minutes and which are attributed to oxygen ion displacement from (to) the HfO_2 layer and subsequent oxidation (reduction) of Ni and Co as a function of the gate voltage [10]. In the present case the notion of a migration of oxygen species towards the Co/HfO_2 interface is well supported by the observed partial surface oxidation of Co, however, a different scenario seems to be at play at the Pt/Co interface and even down to the SiO_2/Pt interface. According to the PNR analysis ion groups, potentially including OH^- or O^{-2} are likely to migrate towards the Pt/Co interface and into the Pt layer to induce a partial oxidation of Co and the anchoring of neutral species that are no longer affected by E-fields. This makes the E-field effect asymmetric with respect to the gate voltage sign and also irreversible which is in good agreement with the

experimental observations.
These important E-field induced chemical and structural rearrangements at the Pt/Co interface are thought to be responsible for the E-field induced reduction of DMI. As it is well known, surface DMI is largely determined by the structure of the interfaces between the magnetic material and the interaction with a heavy metal plays a particularly important role [43, 45]. In addition, the analysis of the SLD profile leads to the conclusion that the structural changes responsible for the expansion of the Pt layer seem to take place at the SiO_2/Pt interface. The neutron SLD profile does not show marked new features at the relatively sharp Pt/Co interface, while the SiO_2/Pt interface becomes increasingly blurred after E-field exposure which could also give rise to strain related effects that could impact DW motion and pinning (see supplementary information [19]).
Another interesting aspect to highlight is the changes taking place between the as-grown sample and the sample biased for 1 minute. The reported decrease in DMI takes place simultaneously with a marked strengthening of PMA. The appearance of PMA is attributed mostly to a gentle oxidation of the Co at the Co/HfO_2 interface. An under/overoxidation of Co is known to decrease PMA [36] while an optimal degree of oxidation can provide the maximum PMA which is here achieved in the vicinity of a biasing time of 1-2 min. Recent studies [44] have shown that the oxidation of the Co surface produces changes in PMA and DMI that follow the same trend. In the present study, D is observed to decrease monotonically showing not to be necessarily linked to the variations in PMA in this short bias time range. This points at the fact that the observed changes in DMI are dominated by the contribution from the Pt/Co interface rather than by those at the Co/HfO_2 interface. As mentioned, an important contribution to DMI is defined at the interface with a heavy metal with high spin orbit coupling [44, 45] and E-field induced ion migration towards the Pt/Co interface can only produce a decrease in DMI, unlike the simultaneous E-field induced oxidation of the top Co interface that can help reaching the optimum level of oxygen content leading to a higher PMA.

VI. CONCLUSION

We have shown an E-field induced non-volatile modification of PMA and DMI in Pt/Co/HfO_2 IL structures. The effects observed are cumulative in time and are attributed to a potential OH^- migration, recombination and anchoring at interfaces in the presence of a negative gate voltage. IL gating allows to permanently modify D, H_K and M_s and to subsequently remove the IL gate for further use of the modified film in any fabrication process. Therefore, this constitutes an interesting method to achieve post-growth PMA and DMI tuning over large scales which can be done in ambient conditions and at room temperature. This method can make post-growth material design possible without the demanding technical requirements of methods like ion irradiation or plasma oxidation which usually need complex plasma/UHV systems. This large and time cumulative modulation of DMI and magnetic anisotropy allows for the use of E-fields by IL gating not only for local control in nanodevices but also as a simple and low-cost tool for post-growth material design.
Further developements are envisioned for this system, specially concerning the reversibility of the E-field effects, by exploring short bias times in the window between 0 and 1 minutes. In addition, valuable information concerning the different DMI contributions coming from the Pt/Co and Co/HfO_2 interfaces could be further explored by controlling the penetration depth of the ions. Interesting perspectives are also to be expected by exploiting the memristive capabilities of HfO_2.

Acknowledgments

We gratefully acknowledge financial support from the European Union FP7 program (ITN WALL No. 608031), the French national research agency (ELECSPIN) as well as from the 2017 Jean d'Alembert Research Fellowship, University of Paris-Saclay excellence initiative. This work was also supported by a public grant overseen by the French National Research Agency (ANR) as part of the 'Investissements d'Avenir' program (Labex NanoSaclay, reference: ANR-10-LABX-0035).

L. H. D. and Y. T. L. contributed equally to this work.

[1] M. Weisheit, S. Fahler, A. Marty, Y. Souche, C. Poinsignon, and D. Givord, Electric Field-Induced Modification of Magnetism in Thin-Film Ferromagnets, Science 315, 349 (2007).
[2] W.-G. Wang, M. Li, S. Hageman, and C. L. Chien, Electric-field assisted switching in magnetic tunnel junctions, Nature Materials 11, 64 (2012).
[3] S. S. P. Parkin, M. Hayashi, and L. Thomas, Magnetic Domain-Wall Racetrack Memory, Science 320, 190 (2008).

[4] A. Thiaville, S. Rohart, É. Jué, V. Cros, and A. Fert, Dynamics of Dzyaloshinskii domain walls in ultrathin magnetic films, EPL (Europhysics Letters) 100, 57002 (2012).

[5] A. Rajanikanth, T. Hauet, F. Montaigne, S. Mangin, and S. Andrieu, Magnetic anisotropy modified by electric field in V/Fe/MgO(001)/Fe epitaxial magnetic tunnel junction, Applied Physics Letters 103, 062402 (2013).

[6] U. Bauer, L. Yao, A. J. Tan, P. Agrawal, S. Emori, H. L. Tuller, S. van Dijken, and G. S. D. Beach, Magneto-ionic control of interfacial magnetism, Nature Materials 14, 174 (2015).

[7] Y. T. Liu, S. Ono, G. Agnus, J.-P. Adam, S. Jaiswal, J. Langer, B. Ocker, D. Ravelosona, and L. Herrera Diez, Electric field controlled domain wall dynamics and magnetic easy axis switching in liquid gated CoFeB/MgO films, Journal of Applied Physics 122, 133907 (2017).

[8] A. Bernand-Mantel, L. Herrera-Diez, L. Ranno, S. Pizzini, J. Vogel, D. Givord, S. Auffret, O. Boulle, I. M. Miron, and G. Gaudin, Electric-field control of domain wall nucleation and pinning in a metallic ferromagnet, Applied Physics Letters 102, 122406 (2013).

[9] U. Bauer, S. Emori, and G. S. D. Beach, Voltage-controlled domain wall traps in ferromagnetic nanowires, Nature Nanotechnology 8, 411 (2013).

[10] X. Zhou, Y. Yan, M. Jiang, B. Cui, F. Pan, and C. Song, Role of Oxygen Ion Migration in the Electrical Control of Magnetism in Pt/Co/Ni/HfO_2 Films, The Journal of Physical Chemistry C 120, 1633 (2016).

[11] D. A. Gilbert, A. J. Grutter, E. Arenholz, K. Liu, B. J. Kirby, J. A. Borchers, and B. B. Maranville, Structural and magnetic depth profiles of magneto-ionic heterostructures beyond the interface limit, Nature Communications 7, (2016).

[12] D. A. Gilbert, J. Olamit, R. K. Dumas, B. J. Kirby, A. J. Grutter, B. B. Maranville, E. Arenholz, J. A. Borchers, and K. Liu, Controllable positive exchange bias via redox-driven oxygen migration, Nature Communications 7, (2016).

[13] A. J. Tan, M. Huang, C. O. Avci, F. Büttner, M. Mann, W. Hu, C. Mazzoli, S. Wilkins, H. L. Tuller, and G. S. D. Beach, Magneto-ionic control of magnetism using a solid-state proton pump, Nature Materials 18, 35 (2019).

[14] T. Srivastava, M. Schott, R. Juge, V. Kikov, M. Belmeguenai, Y. Roussigné, A. Bernand-Mantel, L. Ranno, S. Pizzini, S.-M. Chérif, A. Stashkevich, S. Auffret, O. Boulle, G. Gaudin, M. Chshiev, C. Baraduc, and H. Béa, Large-Voltage Tuning of Dzyaloshinskii-Moriya Interactions: A Route toward Dynamic Control of Skyrmion Chirality, Nano Letters 18, 4871 (2018).

[15] T. Koyama, Y. Nakatani, J. Ieda, and D. Chiba, Electric field control of magnetic domain wall motion via modulation of the Dzyaloshinskii-Moriya interaction, Science Advances 4, eaav0265 (2018).

[16] M. Schott, A. Bernand-Mantel, L. Ranno, S. Pizzini, J. Vogel, H. Béa, C. Baraduc, S. Auffret, G. Gaudin, and D. Givord, The Skyrmion Switch: Turning Magnetic Skyrmion Bubbles on and off with an Electric Field, Nano Letters 17, 3006 (2017).

[17] R. Mishra, F. Mahfouzi, D. Kumar, K. Cai, M. Chen, X. Qiu, N. Kioussis, and H. Yang, Electric-field control of spin accumulation direction for spin-orbit torques, Nature Communications 10, (2019).

[18] S. Ono, S. Seki, R. Hirahara, Y. Tominari, and J. Takeya, High-mobility, low-power, and fast-switching organic field-effect transistors with ionic liquids, Appl. Phys. Lett. 92, 103313 (2008).

[19] See Supplemental Material at [xxxxxxxxx] for more details on sample growth, reversibility, BLS, XPS, XAS and PNR measurements as well as for more information on the obtention of the exchange stiffness constant A and micromagnetics simulations.

[20] M. Belmeguenai, J.-P. Adam, Y. Roussigné, S. Eimer, T. Devolder, J.-V. Kim, S. M. Cherif, A. Stashkevich, and A. Thiaville, Interfacial Dzyaloshinskii-Moriya interaction in perpendicularly magnetized Pt/Co/AlO_x ultrathin films measured by Brillouin light spectroscopy, Physical Review B 91, (2015).

[21] R. Soucaille, M. Belmeguenai, J. Torrejon, J.-V. Kim, T. Devolder, Y. Roussign, S.-M. Chrif, A. A. Stashkevich, M. Hayashi, and J.-P. Adam, Probing the Dzyaloshinskii-Moriya interaction in CoFeB ultrathin films using domain wall creep and Brillouin light spectroscopy, Physical Review B 94, (2016).

[22] S.-G. Je, D.-H. Kim, S.-C. Yoo, B.-C. Min, K.-J. Lee, and S.-B. Choe, Asymmetric magnetic domain-wall motion by the Dzyaloshinskii-Moriya interaction, Physical Review B 88, (2013).

[23] H. T. Nembach, J. M. Shaw, M. Weiler, E. Jué, and T. J. Silva, Linear relation between Heisenberg exchange and interfacial DzyaloshinskiiMoriya interaction in metal films, Nature Physics 11, 825 (2015).

[24] C. A. F. Vaz, J. A. C. Bland, and G. Lauhoff, Magnetism in ultrathin film structures, Reports on Progress in Physics 71, 056501 (2008).

[25] T. Ha Pham, J. Vogel, J. Sampaio, M. Vaatka, J.-C. Rojas-Sánchez, M. Bonfim, D. S. Chaves, F. Choueikani, P. Ohresser, E. Otero, A. Thiaville, and S. Pizzini, Very large domain wall velocities in Pt/Co/GdOx and Pt/Co/Gd trilayers with Dzyaloshinskii-Moriya interaction, EPL (Europhysics Letters) 113, 67001 (2016).

[26] C. Eyrich, W. Huttema, M. Arora, E. Montoya, F. Rashidi, C. Burrowes, B. Kardasz, E. Girt, B. Heinrich, O. N. Mryasov, M. From, and O. Karis, Exchange stiffness in thin film Co alloys, Journal of Applied Physics 111, 07C919 (2012).

[27] K. Shahbazi, J.-V. Kim, H. T. Nembach, J. M. Shaw, A. Bischof, M. D. Rossell, V. Jeudy, T. A. Moore, and C. H. Marrows, Domain-wall motion and interfacial Dzyaloshinskii-Moriya interactions in Pt/Co/Ir(t Ir)/Ta multilayers, Physical Review B 99, (2019).

[28] P. J. Metaxas, J. P. Jamet, A. Mougin, M. Cormier, J. Ferré, V. Baltz, B. Rodmacq, B. Dieny, and R. L. Stamps, Creep and Flow Regimes of Magnetic Domain-Wall Motion in Ultrathin Pt / Co / Pt Films with Perpendicular Anisotropy, Physical Review Letters 99, (2007).

[29] K. Yamada, J.-P. Jamet, Y. Nakatani, A. Mougin, A. Thiaville, T. Ono, and J. Ferré, Influence of Instabilities on High-Field Magnetic Domain Wall Velocity in (Co/Ni) Nanostrips, Applied Physics Express 4, 113001 (2011).

[30] L. H. Diez, M. Voto, A. Casiraghi, M. Belmeguenai, Y. Roussign, G. Durin, A. Lamperti, R. Mantovan, V. Sluka, V. Jeudy, Y. T. Liu, A. Stashkevich, S. M. Chrif, J. Langer, B. Ocker, L. Lopez-Diaz, and D. Ravelosona, Enhancement of the Dzyaloshinskii-Moriya interaction and domain wall velocity through interface intermixing in Ta/CoFeB/MgO, Phys. Rev. B 99, 054431 (2019).

[31] Y. Yoshimura, K.-J. Kim, T. Taniguchi, T. Tono, K. Ueda, R. Hiramatsu, T. Moriyama, K. Yamada, Y.

Nakatani, and T. Ono, Soliton-like magnetic domain wall motion induced by the interfacial DzyaloshinskiiMoriya interaction, Nature Physics 12, 157 (2016).

[32] S. Moretti, M. Voto, and E. Martinez, Dynamical depinning of chiral domain walls, Phys. Rev. B 96, 054433 (2017).

[33] T. J. Regan, H. Ohldag, C. Stamm, F. Nolting, J. Lüning, J. Stöhr, and R. L. White, Chemical effects at metal/oxide interfaces studied by x-ray-absorption spectroscopy, Physical Review B 64, (2001).

[34] B. Liu, M. M. van Schooneveld, Y.-T. Cui, J. Miyawaki, Y. Harada, T. O. Eschemann, K. P. de Jong, M. U. Delgado-Jaime, and F. M. F. de Groot, In-Situ 2p3d Resonant Inelastic X-ray Scattering Tracking Cobalt Nanoparticle Reduction, The Journal of Physical Chemistry C 121, 17450 (2017).

[35] C. T. Chen, Y. U. Idzerda, H.-J. Lin, N. V. Smith, G. Meigs, E. Chaban, G. H. Ho, E. Pellegrin, and F. Sette, Experimental Confirmation of the X-Ray Magnetic Circular Dichroism Sum Rules for Iron and Cobalt, Physical Review Letters 75, 152 (1995).

[36] A. Manchon, C. Ducruet, L. Lombard, S. Auffret, B. Rodmacq, B. Dieny, S. Pizzini, J. Vogel, V. Uhl, M. Hochstrasser, and G. Panaccione, Analysis of oxygen induced anisotropy crossover in Pt/Co/MOx trilayers, Journal of Applied Physics 104, 043914 (2008).

[37] C. R. Parkinson, M. Walker, and C. F. McConville, Reaction of atomic oxygen with a Pt() surface: chemical and structural determination using XPS, CAICISS and LEED, Surface Science 545, 19 (2003).

[38] B. J. Kirby, P. A. Kienzle, B. B. Maranville, N. F. Berk, J. Krycka, F. Heinrich, and C. F. Majkrzak, Phase-sensitive specular neutron reflectometry for imaging the nanometer scale composition depth profile of thin-film materials, Current Opinion in Colloid & Interface Science 17, 44 (2012).

[39] D. A. Gilbert, A. J. Grutter, P. D. Murray, R. V. Chopdekar, A. M. Kane, A. L. Ionin, M. S. Lee, S. R. Spurgeon, B. J. Kirby, B. B. Maranville, A. T. NDiaye, A. Mehta, E. Arenholz, K. Liu, Y. Takamura, and J. A. Borchers, Ionic tuning of cobaltites at the nanoscale, Physical Review Materials 2, (2018).

[40] C. Driemeier, E. P. Gusev, and I. J. R. Baumvol, Room temperature interactions of water vapor with HfO2 films on Si, Applied Physics Letters 88, 201901 (2006).

[41] C. Driemeier, R. M. Wallace, and I. J. R. Baumvol, Oxygen species in HfO2 films: An in situ x-ray photoelectron spectroscopy study, Journal of Applied Physics 102, 024112 (2007).

[42] T. Hirai, T. Koyama, A. Obinata, Y. Hibino, K. Miwa, S. Ono, M. Kohda, and D. Chiba, Control of magnetic anisotropy in Pt/Co system using ionic liquid gating, Applied Physics Express 9, 063007 (2016).

[43] H. Yang, A. Thiaville, S. Rohart, A. Fert, and M. Chshiev, Anatomy of Dzyaloshinskii-Moriya Interaction at Co/Pt Interfaces, Physical Review Letters 115, (2015).

[44] D. de S. Chaves, F. Ajejas, V. Kikov, J. Vogel, and S. Pizzini, Oxidation dependence of the Dzyaloshinskii-Moriya interaction in Pt / Co / MO_x trilayers (M = Al or Gd), Phys. Rev. B 99, 144404 (2019).

[45] J. Torrejon, J. Kim, J. Sinha, S. Mitani, M. Hayashi, M. Yamanouchi, and H. Ohno, Interface control of the magnetic chirality in CoFeB/MgO heterostructures with heavy-metal underlayers, Nature Communications 5, (2014).

[46] P. A. Kienzle, J. Krycka, N. Patel, and I. Sahin, Computer software BUMPS. University of Maryland, College Park, MD, (2011).